

Holistic discretisation ensures fidelity to Burgers' equation

A. J. Roberts*

March 24, 2000

Abstract

I analyse a generalised Burgers' equation to introduce a new method of spatial discretisation. The analysis is based upon centre manifold theory so we are assured that the discretisation accurately models the dynamics and may be constructed systematically. The trick to the application of centre manifold theory is to divide the physical domain into small elements by introducing insulating internal boundaries which are later removed. Burgers' equation is used as an example to show how the concepts work in practise. The resulting finite difference models are shown to be significantly more accurate than conventional discretisations, particularly for highly nonlinear dynamics. This centre manifold approach treats the dynamical equations as a whole, not just as the sum of separate terms—it is holistic. The techniques developed here may be used to accurately model the nonlinear evolution of quite general spatio-temporal dynamical systems.

*Dept Maths & Computing, University of Southern Queensland, Toowoomba, Queensland 4352, AUSTRALIA. <mailto:aroberts@usq.edu.au>

```
@article{Roberts98a,
  author = {A.~J. Roberts},
  title = {Holistic discretisation ensures fidelity to {Burgers'}},
  year = 2001,
  journal = {Applied Numerical Modelling},
  volume = 37,
  pages = {371--396},
  url = {http://arXiv.org/abs/chao-dyn/9901011},
}
```

Contents

1	Introduction	3
2	Centre manifold theory underpins the fidelity	11
3	Numerical comparisons show the effectiveness	16
4	Higher order approximations are more accurate	22
5	Nonlinear stability of the discretisations	27
6	Simplify models with a coordinate transform	31
7	Conclusion	34
A	Global discretisations converge to spectral accuracy	36
B	Computer algebra develops the approximations	42

1 Introduction

I introduce a new approach to discretisation by illustrating the concepts and analysis on the definite example of a generalised Burgers' equation. The aim of this approach is to use dynamical systems analysis to improve the accuracy, stability and efficiency of numerical discretisations. As a first implementation we study a variant to Burgers' equation in one spatial dimension. The analysis reported herein is largely computational experiment on specific examples to explore how the ideas actually work in a specific example.

In some non-dimensional form we take the following partial differential equation (PDE) to govern the evolution of $u(x, t)$:

$$\frac{\partial u}{\partial t} + \alpha u \frac{\partial u}{\partial x} = \frac{\partial^2 u}{\partial x^2} - \beta u^3. \quad (1)$$

This example equation, which includes the mechanisms of dissipation, u_{xx} , and nonlinear advection/steepening, $\alpha u u_x$, generalises Burgers' equation by also including a nonlinear damping ($\beta > 0$) or reacting ($\beta < 0$) term βu^3 (as in [19]). Consider implementing the method of lines by discretising in x and integrating in time as a set of ordinary differential equations, sometimes called a semi-discrete scheme [10, 12, e.g.]. I only address the spatial discretisation of (1) and treat the resulting set of ordinary differential equations as a continuous time dynamical system. A finite difference approximation to the spatial structure of (1) on a regular grid in x is straightforward, say $x_j = jh$ for some constant grid spacing h . For example, the linear term

$$\frac{\partial^2 u}{\partial x^2} = \frac{u_{j+1} - 2u_j + u_{j-1}}{h^2} + \mathcal{O}(h^2),$$

where u_j is the value of u at the grid points x_j . However, there are differing valid alternatives for the nonlinear term uu_x : two possibilities are

$$u \frac{\partial u}{\partial x} = \frac{u_j(u_{j+1} - u_{j-1})}{2h} + \mathcal{O}(h^2) = \frac{u_{j+1}^2 - u_{j-1}^2}{4h} + \mathcal{O}(h^2);$$

and a third is the 1 : 2 mix of the above two suggested by Fornberg [13] and used to improve stability [10, e.g.]. Which is better? The answer depends upon how the discretisation of the nonlinearity interacts with the dynamics of other terms. The traditional approach of considering the discretisation of each term separately does not tell us. Instead, in order to find the best discretisation we should consider the influence of all terms in the equation in a holistic approach.

Centre manifold theory has appropriate characteristics to do this (see the book by Carr [2] for a good introduction). It addresses the evolution of a dynamical system in a neighbourhood of a marginally stable fixed point; based upon the linear dynamics the theory guarantees that an accurate low-dimensional description of the nonlinear dynamics may be deduced. The theory is a powerful tool for the modelling of complex dynamical systems [3, 4, 28, 29, 15, e.g.] such as dispersion [41, 27, 45, e.g.], thin fluid films [5, 34, 37, e.g.] and other applications discussed in the review [35]. Here we place the discretisation of a nonlinear PDE such as (1) within the purview of centre manifold theory by the following artifice (such mathematical trickery proved effective in thin fluid flows [34]). Introduce a homotopy parameter γ , $0 \leq \gamma \leq 1$: at the midpoints of the grid, $x = (j + 1/2)h$, insert artificial boundaries which are “insulating” when $\gamma = 0$, but which couple adjacent elements for $\gamma \neq 0$ so that when $\gamma = 1$ the internal boundary conditions ensure sufficient continuity to recover the original problem. In essence this divides the domain into equi-sized elements centred upon each grid point, say the domain is partitioned into m elements. For (1) we may use

$$\frac{\partial u^+}{\partial x} = \frac{\partial u^-}{\partial x}, \quad (1 - \gamma) \frac{h}{2} \left(\frac{\partial u^+}{\partial x} + \frac{\partial u^-}{\partial x} \right) = \gamma (u^+ - u^-), \quad (2)$$

where u^+ is just to the right of a midpoint and u^- to the left. When $\gamma = 1$ these reduce to conditions ensuring appropriate continuity between adjacent elements. When $\gamma = 0$ they reduce to conditions equivalent to the insulating

$$\frac{\partial u^+}{\partial x} = \frac{\partial u^-}{\partial x} = 0.$$

We then treat terms multiplied by γ as “nonlinear” perturbations to the insulated dynamics. Then in the “linear” dynamics governed by

$$\frac{\partial u}{\partial t} = \frac{\partial^2 u}{\partial x^2},$$

the field u in each element evolves exponentially quickly (in a time $\mathcal{O}(h^2)$) to a constant value, say $u = u_j$ in the j th element (the particular value depends upon the initial conditions). But in the presence of the perturbative influences of the nonlinear terms and the coupling between the elements when $\gamma \neq 0$, the values u_j associated with each element will evolve in time. This picture is the basis of centre manifold theory which is applied in Section 2 to assure three things:

- the existence of an m dimensional centre manifold parametrised by u_j (m is the number of grid points or elements);
- the relevance of the m dimensional dynamics as an accurate and stable model of the original dynamics (1);
- and that we may approximate the shape of the centre manifold and the evolution thereon by approximately solving an associated differential equation.

These dynamics on the centre manifold form a finite difference approximation.

It might be argued that the dynamics of Burgers’ equation at $\gamma = 1$ is completely unrelated to that of the derived model which is based

upon asymptotics about $\gamma = 0$. This is not necessarily so: Taylor series are summed within their radius of convergence; finite differences are used at finite grid spacing h even though they are primarily justified by consistency in the limit $h \rightarrow 0$. We routinely use asymptotic expansions at finite values of a notionally small parameter. The practical issue here is whether the expansion converges at $\gamma = 1$, see the Appendix A to see convergence to a global discretisation of Burgers equation and see [34] for analogous convergence to a model of thin fluid films. However, here I just match the discretisation with those obtained from the traditional discretisation obtained in the limit $h \rightarrow 0$. That the modelling process satisfies these two independent asymptotic limits seems to provide good support for the proposed approach.

For example, the analysis in Section 3 of the generalised Burgers' equation (1) favours the discretisation

$$\begin{aligned} \dot{u}_j + \alpha u_j \left[\frac{u_{j+1} - u_{j-1}}{2h} - \frac{\alpha u_j}{12} (u_{j+1} - 2u_j + u_{j-1}) \right] \\ \approx \frac{u_{j+1} - 2u_j + u_{j-1}}{h^2} \\ - \frac{\beta}{24} \left(u_{j-1}^3 + 3u_{j-1}u_j^2 + 16u_j^3 + 3u_{j+1}u_j^2 + u_{j+1}^3 \right), \end{aligned} \quad (3)$$

as an early approximation (\dot{u}_j denotes du_j/dt). Provided the initial conditions are not too extreme, centre manifold theory assures us that such a discretisation models the dynamics of (1) to errors $\mathcal{O}(\|u\|^4)$. Observe that it seems best to discretise the nonlinear uu_x terms directly, but that there is a nonlinear correction involving the second difference which is interpreted (see §5) either as a nonlinear upwind differencing correction or as a nonlinearly enhanced dissipation. Further, the cubic nonlinearity is discretised in a non-obvious complicated form. Simplifications to the algebraic form of such an approximation are discussed in Section 6 using near identity coordinate transformations to reparametrise the centre manifold. However, there we find the possible simplifications are not very significant so I prefer to develop models in

terms of the clearly defined grid point values $u_j = u(x_j)$.

This approach to the discretisation, at least for Burgers' equation explored here, improves stability. For example, following Foias *et al* [10, §2.1] we briefly consider the dynamics of $\sigma(t) = h(u_1 + u_2)$ and $\zeta(t) = h(u_1 - u_2)$ when $u_0 = u_3 = 0$ for the discretisation of the pure Burgers' equation, $\beta = 0$ in (3). Further analysis is given in Section 5. Without the nonlinear correction to the advection term, that is using $uu_x \approx u_j(u_{j+1} - u_{j-1})/2h$, the amplitudes σ and ζ evolve according to

$$h^2\dot{\sigma} = -\sigma, \quad h^2\dot{\zeta} = -3\zeta + \frac{\alpha}{4}(\zeta^2 - \sigma^2). \quad (4)$$

As found by Foias *et al.* [10] for the Kuramoto-Sivashinsky equation, whereas $\sigma \rightarrow 0$ exponentially quickly, as does ζ if it is sufficiently small, the fixed point at $\zeta = 12/\alpha$ flags a blow-up in ζ in finite time for a range of initial conditions. This blow-up does not happen using the discretisation of uu_x in (3). The corresponding equations for σ and ζ are then

$$h^2\dot{\sigma} = -\sigma \left[1 + \frac{\alpha^2}{48}(\sigma^2 + 7\zeta^2) + \frac{\beta}{24}(5\sigma^2 + 12\zeta^2) \right], \quad (5)$$

$$h^2\dot{\zeta} = -3\zeta + \frac{\alpha}{4}(\zeta^2 - \sigma^2) - \frac{\alpha^2}{48}\zeta(3\zeta^2 + 5\sigma^2) - \frac{\beta}{8}\zeta(\zeta^2 + 4\sigma^2). \quad (6)$$

Thus for $\beta \geq -\alpha^2/10$ it is readily apparent that $\sigma \rightarrow 0$ exponentially quickly but now so also does ζ for *all* initial conditions as there are no spurious fixed points. The discretisation (3), obtained systematically via a centre manifold analysis, is nonlinearly stable when other discretisations are not.

The discretisation (3) is just a low-order approximation, centre manifold theory provides systematic corrections. For example, Equation (3) is obtained from terms linear in the element coupling γ . Analysis including quadratic terms in γ leads to the fourth-order accurate model discussed in Section 4. Analysis to higher orders in the nonlinearity,

discussed in Section 3, shows higher order corrections to the discretisation of the nonlinear terms and interestingly also incorporates effects from the interaction of the different nonlinearities.

Maintaining fidelity with Burgers' equation (1) is sought by using centre manifold theory to construct approximations based upon the principle of capturing an exponentially attractive manifold of solutions. Jones & Stuart [22] argue that quite generally there exist good approximations to attractive inertial manifolds. The challenge we address here is to actually construct effective approximations. Margolin & Jones [24] have previously applied inertial manifold ideas to discretisations of Burgers' equation. However, they used just two basis functions on each element and invoked the adiabatic approximation for time derivatives of "slaved" modes. Here I allow arbitrarily convoluted dependence within each element and include all effects of time variations. The methodology presented here provides a more systematic approach to discretisation.

Inertial manifolds were developed to faithfully capture the long-term, low-dimensional dynamics of dissipative PDE's [43]. Most efforts to actually construct approximations to an inertial manifold have been based upon the so-called nonlinear Galerkin method of Roberts [33], Foias et al. [9] and Marion & Temam [25] (though Jolly [19] based a construction upon the unstable manifolds of fixed points). Not only do proofs of existence rely on large spectral gaps [43, Eqn. (10), e.g.], but the construction relies on finding the *global* eigenfunctions of the linear dynamics. This is so for the variants explored by Jolly et al. [20], for the case when the global inertial manifold is parametrised by discrete points, see [12], §A and §6, and also for the more efficient post-processing Galerkin method of García-Archilla et al. [16]. The nonlinear Galerkin method, though appealing and though improving convergence [21, e.g.], is impractical in applications with possibly varying coefficients and complicated boundaries. In contrast, the approach proposed here is based purely upon the *local* dynamics on small elements

while maintaining, as do inertial manifolds, fidelity with the solutions of the original PDE. A difference is that the analysis does not rest upon the exponential decay towards the global attractor, but upon the exponential decay of the small, subgrid structures in each local element. One favourable consequence is that here there is no need to invoke a highly restrictive spectral gap condition [12, Eqn. (5.4) e.g.]. The very first sentence in García-Archilla et al. [17] says “Finite-element methods seem not to have benefited as much as spectral methods from some of the recent advances in the Dynamical Systems approach to partial differential equations”. Here I introduce an innovation in the application of dynamical systems theory to the construction of element based discretisations.

Further, the extension to discretisations in higher spatial dimensions is straightforward and the resultant model much less costly to use than a global description of an inertial manifold. Consider, as a simple example, the class of diffusive PDE’s, including the Brusselator [17, §3] for example,

$$\frac{\partial u}{\partial t} = \nabla^2 u + f(u, \nabla u),$$

where f represents nonlinear reaction or advection effects. After tessellating space into finite elements the fundamental problem in constructing a model with the approach here is simply to solve Poisson’s equation with forced Neumann boundary conditions on each element. Although this sub-grid problem may itself need to be done numerically, in the simplest case of a regular tessellation it need only be done once for each term in the model, just like the computation of the interaction terms in a traditional finite element approximation [42, e.g.]. Thus in d -dimensions with grid spacing $h \propto 1/m$ and a discretisation of width k in space we expect each of m^d elements to involve the k^d amplitudes of the neighbouring elements. In a model developed to order p interactions between the amplitudes, for example (3) is cubic $p = 3$, expect $k^{p d}$ computations per element and hence a total computational cost propor-

tional to $(k^p m)^d$ operations. However, a corresponding approximation to the evolution on an inertial manifold based upon global modes will involve m^d modes all of which will interact in the order p approximation and so will incur a cost proportional to m^{pd} . In higher dimensions the finite width discretisations corresponding to those developed here will be much cheaper to evaluate.

Computer algebra is an effective tool for constructing the models because of the systematic nature of centre manifold theory [30, 14, 36]. The specific finite difference models presented here were derived by the computer algebra program given in Appendix B. Such a computer algebra program may be straightforwardly modified to model more complicated dynamical systems.

In this work I concentrate upon a proof of the concept of applying centre manifold theory to constructing effective discretisations. To that end we only consider a constant coefficient, one-dimensional problem in an infinite domain or strictly periodic solutions in finite domains. Then all elements of the discretisation are identical by symmetry and the analysis of all elements is simultaneous. However, if physical boundaries to the domain of the PDE are present, then those elements near the physical boundary will need special treatment. There is no need for any new concepts, just an increase in the amount of detail. Similarly the analysis presented here is essentially *local* in space, in contrast to the global nature of the nonlinear Galerkin approximation to inertial manifolds, thus spatially varying problems pose no conceptual problems: if the linear terms have constant coefficients then the model would just involve integrals of the other coefficient functions; whereas if more generally all coefficients vary then local Taylor series expansions of the coefficients will be effective because of the small element size h . The centre manifold approach also sheds an interesting light upon the issue of the initial condition for a finite difference approximation. Earlier work on the issue of initial conditions in general [32, 8, 38] suggests that the initial values for the parameters $u_j(t)$

are not simply the field sampled at the grid points, $u(x_j, 0)$, but some more subtle transform. Preliminary research suggests a leading order approximation is that $u_j(0)$ is the element average of $u(x, 0)$, an approximation which usefully conserves u . Lastly, here we only analyse an autonomous dynamical system, the PDE (1); forcing applied to the PDE may be approximated using the projection obtained for initial conditions [7, 38]. These show that, to avoid integrals over past history, there are more subtleties in projecting the forcing than assumed by Jones *et al* [21] in constructing their inertial manifold. Further research is needed in the above issues and in the application of the theory to higher order PDEs (a preliminary application to the dynamics of Kuramoto-Sivashinsky equation is reported in [23]).

2 Centre manifold theory underpins the fidelity

In this section I describe in detail one way to place the discretisation of PDEs within the purview of centre manifold theory. For definiteness I address the generalised Burgers' equation (1) as an example of a broad class of PDEs.

As introduced earlier, the discretisation is established via an equi-spaced grid of collocation points, $x_j = jh$ say, for some constant spacing h . At midpoints $x_{j+1/2} = (x_j + x_{j+1})/2$ artificial boundaries are introduced with one extra refinement over that discussed in the Introduction:

$$\frac{\partial u^+}{\partial x} = \frac{\partial u^-}{\partial x}, \quad (7)$$

$$(1 - \gamma)\mathcal{A}\frac{h}{2}\left(\frac{\partial u^+}{\partial x} + \frac{\partial u^-}{\partial x}\right) = \gamma(u^+ - u^-), \quad (8)$$

where the introduction of the near identity operator

$$\mathcal{A} = 1 - \frac{h^2}{12} \frac{\partial}{\partial t} + \frac{h^4}{120} \frac{\partial^2}{\partial t^2} - \frac{17h^6}{20160} \frac{\partial^3}{\partial t^3} + \dots, \quad (9)$$

will be explained in Section 4. These boundaries divide the domain into a set of elements, the j th element centred upon x_j and of width h as seen, for example, in Figure 1. A non-zero value of the parameter γ couples these elements together so that when $\gamma = 1$ the PDE is effectively restored over the whole domain. The generalised Burgers' equation (1) with “internal boundary conditions” (7–8) is analysed here to give the discretisation in the interior of the domain.

The application of centre manifold theory is based upon a linear picture of the dynamics. Adjoin the dynamically trivial equation

$$\frac{\partial \gamma}{\partial t} = 0, \quad (10)$$

and consider the dynamics in the extended state space $(u(x), \gamma)$. This is a standard technique used to unfold bifurcations [2, §1.5] or to justify long-wave approximations [31]. Within each element $u = \gamma = 0$ is a fixed point. Linearized about each fixed point, that is to an error $\mathcal{O}(\|u\|^2 + \gamma^2)$, the PDE is

$$\frac{\partial u}{\partial t} = \frac{\partial^2 u}{\partial x^2}, \quad \text{s.t.} \quad \mathcal{A} \left. \frac{\partial u}{\partial x} \right|_{x=x_{j \pm 1/2}} = 0,$$

namely the diffusion equation with essentially insulating internal boundaries. There are thus linear eigenmodes associated independently with each element:

$$\gamma = 0, \quad u \propto \begin{cases} e^{\lambda_n t} \cos[n\pi(x - x_{j-1/2})/h], & x_{j-1/2} < x < x_{j+1/2}, \\ 0, & \text{otherwise,} \end{cases} \quad (11)$$

for $n = 0, 1, \dots$, where the decay rate of each mode is

$$\lambda_n = -\frac{n^2 \pi^2}{h^2}; \quad (12)$$

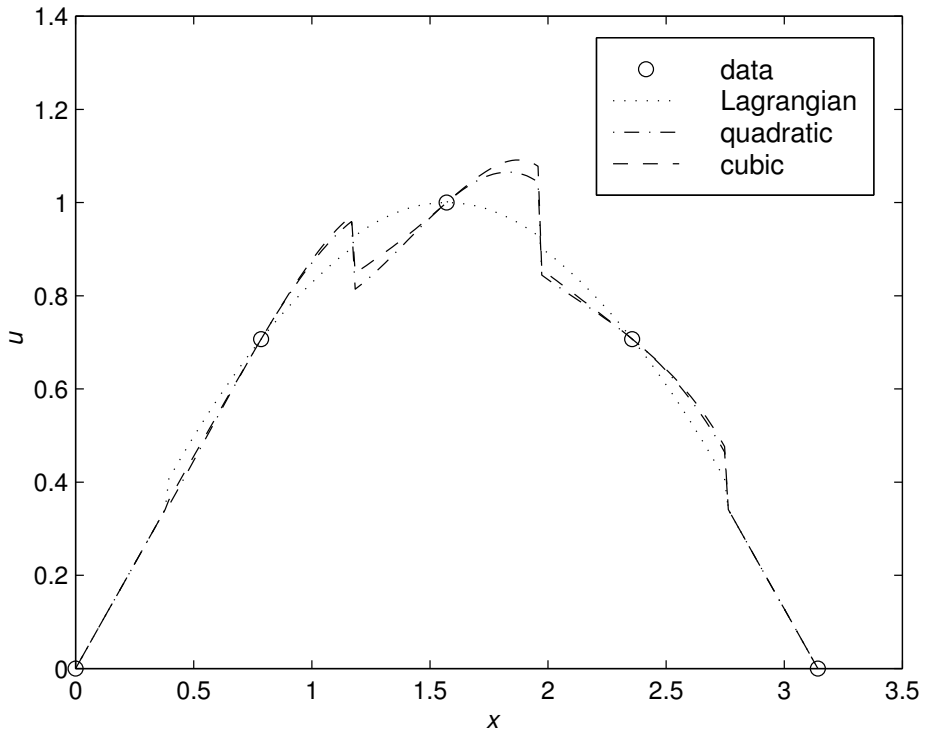


Figure 1: low order approximations (16) to the centre manifold field $u(x)$ within each element centred on each of a fixed set of data points (circles) corresponding to $m = 8$ intervals on $[0, 2\pi)$ (half a period shown) with parameters $\alpha = 6$, $\beta = 0$ and $\gamma = 1$: \cdots , traditional Lagrangian interpolant; $-\cdot-\cdot-$, includes the quadratic effects of the nonlinear advection term, αuu_x ; $-----$, includes the cubic effects of advection.

together with the trivial mode $\gamma = \text{const}$, $u = 0$. In a domain with m elements, evidently all eigenvalues are negative, $-\pi^2/h^2$ or less, except for $m + 1$ zero eigenvalues: 1 associated with each of the m elements and 1 from the trivial (10). Thus, provided the nonlinear terms in (1) are sufficiently well behaved, the existence theorem ([4, p281] or [44, p96]) guarantees that a $m + 1$ dimensional centre manifold \mathcal{M} exists for (1) with (7–10). The centre manifold \mathcal{M} is parametrised by γ and a measure of u in each element, say u_j : using \mathbf{u} to denote the collection of such parameters, \mathcal{M} is written as

$$u(x, t) = v(x; \mathbf{u}, \gamma) . \quad (13)$$

In this the analysis has a very similar appearance to that of finite elements [42, e.g.]; a difference is that here the structure of the solution internal to the element is driven by the PDE rather than being imposed arbitrarily. The existence theorem also asserts that on the centre manifold the parameters u_j evolve deterministically

$$\dot{u}_j = g_j(\mathbf{u}, \gamma) , \quad (14)$$

where g_j is the restriction of (1) and (7–10) to \mathcal{M} . In this approach the parameters of the description of the centre manifold may be anything that sensibly measures the size of u in each element—I simply choose the value of u at the grid points, $u_j = u(x_j, t)$. This provides the necessary amplitude conditions, namely that

$$u_j = v|_{x_j} . \quad (15)$$

The above application of the existence theorem establishes that in principle we may find the dynamics (14) of the interacting elements of the discretisation. A low order approximation is given in (3).

The next outstanding question to answer is: how can we be sure that such a description of the interacting elements does actually *model* the dynamics of the original system (1) with (7–10)? In the development of inertial manifolds by Temam [43] and others, this question is

sometimes phrased as one about the asymptotic completeness of the model, for example see Robinson [40] or Constantin et al [6, Chapt.12–3], and sometimes referred to as exponential tracking [11, e.g.]. Here, the relevance theorem of centre manifolds, [4, p282] or [44, p128], guarantees that all solutions of (1) and (7–10) which remain in the neighbourhood of the origin in $(u(x), \gamma)$ space are exponentially quickly attracted to a solution of the m finite difference equations (14). For practical purposes the rate of attraction is estimated by the leading negative eigenvalue, here $-\pi^2/h^2$. Centre manifold theory also guarantees that the stability near the origin is the same in both the model and the original. Thus the finite difference model will be stable if the original dynamics are stable. After exponentially quick transients have died out, the finite difference equation (14) on the centre manifold accurately models the complete system (1) and (7–10).

The last piece of theoretical support tells us how to approximate the shape of the centre manifold and the evolution thereon. Approximation theorems such as that by Carr & Muncaster [4, p283] assure us that upon substituting the ansatz (13–14) into the original (1) and (7–10) and solving the equations to some order of residual in $\|u\|$ and γ , then \mathcal{M} and the evolution thereon will be approximated with an error to the same order. The catch with this application is that we need to evaluate the approximations at $\gamma = 1$ because it is only then that the artificial internal boundaries are removed. Thus although the order of error estimates do provide assurance, the actual error due to the evaluation at $\gamma = 1$ should be also assessed otherwise. In some applications of such an artificial homotopy I have demonstrated excellent convergence in the parameter γ [34]. Here, as discussed in Section 4, we have crafted the interaction (8) between elements so that low order terms in γ recover the traditional finite difference formula for linear terms. Note that although centre manifold theory “guarantees” useful properties near the origin in $(u(x), \gamma)$ space, because of the need to evaluate the asymptotic expressions at $\gamma = 1$, I have used a weaker term elsewhere, namely “assures”.

3 Numerical comparisons show the effectiveness

We now turn to a detailed description of the centre manifold model for Burgers' equation (1) for various orders of approximation.

The algebraic details of the derivation of the centre manifold model (13–14) is the task of the computer algebra program listed in Appendix B. In an algorithm introduced and explained in [36], the program iteratively corrects an approximation to drive to zero the residuals of the governing differential equation (1) and its boundary conditions (7–8). A key part of the iteration is to solve for corrections v' and g' from the linear diffusion equation within each element

$$\frac{\partial^2 v'}{\partial x^2} = g' + R, \quad \left. \frac{\partial v'}{\partial x} \right|_{x_{j\pm 1/2}} = R_{\pm},$$

where R and R_{\pm} denote the residuals for the current approximation. The initial approximation is simply that in each element $u = u_j$, constant, with $\dot{u}_j = g_j = 0$. The algebraic details of this iteration are largely immaterial so long as the residuals are reduced to zero to some order in $\|u\|$ and γ . This is achieved by the listed computer algebra program, it is included to replace the recording of tedious details of elementary algebra.

The shape of the centre manifold gives the field u as a function of the parameters u_j and the coupling γ . To low-order in $\|u\|$ and γ , and written in terms of the scaled coordinate $\xi = (x - x_j)/h$, the solution field in the j th element is

$$u = u_j + \gamma \left[\frac{u_{j+1} - u_{j-1}}{2} \xi + \frac{u_{j+1} - 2u_j + u_{j-1}}{2} \xi^2 \right] + h\gamma \left[\alpha u_j (u_{j+1} - 2u_j + u_{j-1}) \left(\frac{1}{6} \xi^3 - \frac{1}{8} \xi \right) \right]$$

$$\begin{aligned}
& + h^2 \gamma \left[\alpha^2 u_j^2 (u_{j+1} - 2u_j + u_{j-1}) \left(\frac{1}{24} \xi^4 - \frac{1}{48} \xi^2 \right) \right. \\
& + \beta (u_{j+1}^3 - 3u_{j+1}u_j^2 + 4u_j^3 - 3u_{j-1}u_j^2 + u_{j-1}^3) \left(-\frac{1}{24} \xi^4 - \frac{1}{48} \xi^2 \right) \\
& + \beta (u_{j+1}^3 - 3u_{j+1}u_j^2 + 3u_{j-1}u_j^2 - u_{j-1}^3) \left(-\frac{1}{12} \xi^3 + \frac{1}{48} \xi \right) \\
& \left. - \beta \frac{u_j^2}{8} \left((u_{j+1} - u_{j-1})\xi + (u_{j+1} - 2u_j + u_{j-1})\xi^2 \right) \right] \\
& + \mathcal{O}(\|u\|^4, \gamma^2).
\end{aligned} \tag{16}$$

Observe the first line, when evaluated at $\gamma = 1$, is simply the usual Lagrangian interpolant based upon second order accurate centred differences. As displayed in Figure 1, the second line shows that this field should be modified because of the quadratically nonlinear advection term $\alpha u u_x$; the modification in proportion to the second difference at x_j is reasonable because when u has a local maximum the field must be decreased/increased to the left/right due to the advection to the right of the lower/higher levels of u respectively. Note that the same discretisation for this nonlinear term is obtained here whether we code it as $\alpha u u_x$ or $\alpha (u^2)_x/2$ —the centre manifold is independent of any valid change in the algebraic description of the dynamics. The third line gives the next order correction due to the nonlinear advection, cubic in u , and is also displayed in Figure 1. The fourth, fifth and sixth lines show how the reaction term, βu^3 , modifies u in the element because of its nonlinearly varying effect as a source or sink when the field u itself varies. It might appear odd to introduce the dysfunctional behaviour between elements shown in Figure 1, but centre manifold theory reasonably assures us that it is appropriate for the nonlinear dynamics we wish to model. Indeed, as is seen in Appendix A, the centre manifold field u does acquire the required continuity between elements, shown in Figure 5, when the interactions are developed to higher order in γ . In short, the description of the centre manifold is based upon standard

differencing formulae, but includes effects upon u within each element due to the nonlinear processes that act in the continuum dynamics.

The finite difference model is given by the evolution on the centre manifold. To linear terms in γ but to two orders higher in $\|u\|$ (quintic in $\|u\|$) it is

$$\begin{aligned}
 \dot{u}_j = & \frac{\gamma}{h^2} (u_{j+1} - 2u_j + u_{j-1}) - \frac{\gamma\alpha}{2h} u_j (u_{j+1} - u_{j-1}) - \beta u_j^3 \\
 & + \gamma \left[\frac{\alpha^2}{12} u_j^2 (u_{j+1} - 2u_j + u_{j-1}) \right. \\
 & \quad \left. + \frac{\beta}{24} (-u_{j+1}^3 - 3u_{j+1}u_j^2 + 8u_j^3 - 3u_{j-1}u_j^2 - u_{j-1}^3) \right] \\
 & + h\gamma \left[\frac{\alpha\beta}{8} u_j^3 (u_{j+1} - u_{j-1}) \right] \\
 & + h^2\gamma \left[-\frac{\alpha^4}{720} u_j^4 (u_{j+1} - 2u_j + u_{j-1}) \right. \\
 & \quad + \frac{\alpha^2\beta}{5760} u_j^2 (9u_{j+1}^3 - 113u_{j+1}u_j^2 + 208u_j^3 - 113u_{j-1}u_j^2 + 9u_{j-1}^3) \\
 & \quad + \frac{\beta^2}{1920} (-21u_{j+1}^5 + 6u_{j+1}^3u_j^2 + 7u_{j+1}u_j^4 + 16u_j^5 \\
 & \quad \quad \left. + 7u_{j-1}u_j^4 + 6u_{j-1}^3u_j^2 - 21u_{j-1}^5) \right] \\
 & + \mathcal{O}(\|u\|^6, \gamma^2).
 \end{aligned} \tag{17}$$

The first line recorded here, when evaluated for $\gamma = 1$, is just the classic second-order finite difference equation for the generalised Burgers' equation (1). The second line starts accounting systematically for the variations in the field u within each element and how they affect the evolution through the nonlinear terms. The approximation formed by the first three lines is that reported in the Introduction as (3). The fourth and further lines above, through $\alpha\beta$ and $\alpha^2\beta$ effects, show that this approach also accounts for interaction between

the nonlinear terms in the PDE in the finite difference approximation. Finite difference equations derived via this approach holistically model all the interacting dynamics of the entire PDE.

To show the effectiveness of the approach I compare predictions of the finite difference model (17) to exact solutions of Burgers' equation (1) with $\beta = 0$. Exact solutions are obtained via the Cole-Hopf transformation $u = -(2/\alpha)\phi_x/\phi$ by choosing $\phi(x, t)$ to satisfy the diffusion equation $\phi_t = \phi_{xx}$. For example, here I choose 2π -periodic functions

$$\phi = \frac{14}{\sqrt{t_0}} e^{-\pi^2/4t_0} + \sum_k \frac{1}{\sqrt{t+t_0}} \exp \left[-\frac{(x - k2\pi)^2}{4(t+t_0)} \right],$$

with $t_0 = \pi/(4\sqrt{\alpha})$, chosen so that the initial state $u(x, 0)$ is a rough approximation to $\sin(x)$. Note that consequently $\|u(x, 0)\| \approx 1$ and thus varying the coefficient α varies the importance of the nonlinear advection. Choosing m intervals on $[0, 2\pi)$ gives an element length $h = 2\pi/m$ and grid points $x_j = jh$ for $j = 0, \dots, m-1$. Because of the antisymmetry in $u(x, t)$ about $x = k\pi$, I only display the interval $[0, \pi]$. With $\beta = 0$, there are three different approximations from (17), with $\gamma = 1$, depending upon where the expansion is truncated in $\|u\|$ (or equivalently in α):

$$\begin{aligned} \dot{u}_j \approx & \frac{1}{h^2} (u_{j+1} - 2u_j + u_{j-1}) - \frac{\alpha}{2h} u_j (u_{j+1} - u_{j-1}) \\ & + \frac{\alpha^2}{12} u_j^2 (u_{j+1} - 2u_j + u_{j-1}) \\ & - h^2 \frac{\alpha^4}{720} u_j^4 (u_{j+1} - 2u_j + u_{j-1}). \end{aligned} \quad (18)$$

Just the first line forms a model with quadratic nonlinearities obtained directly from the advection (a normal finite difference approximation), the first two lines form a model with cubic nonlinearities, errors $o(\|u\|^3)$ or equivalently $o(\alpha^2)$ errors, and all shown terms form the quintic model, with $o(\|u\|^5)$ or $o(\alpha^4)$ errors. The solutions of these models over

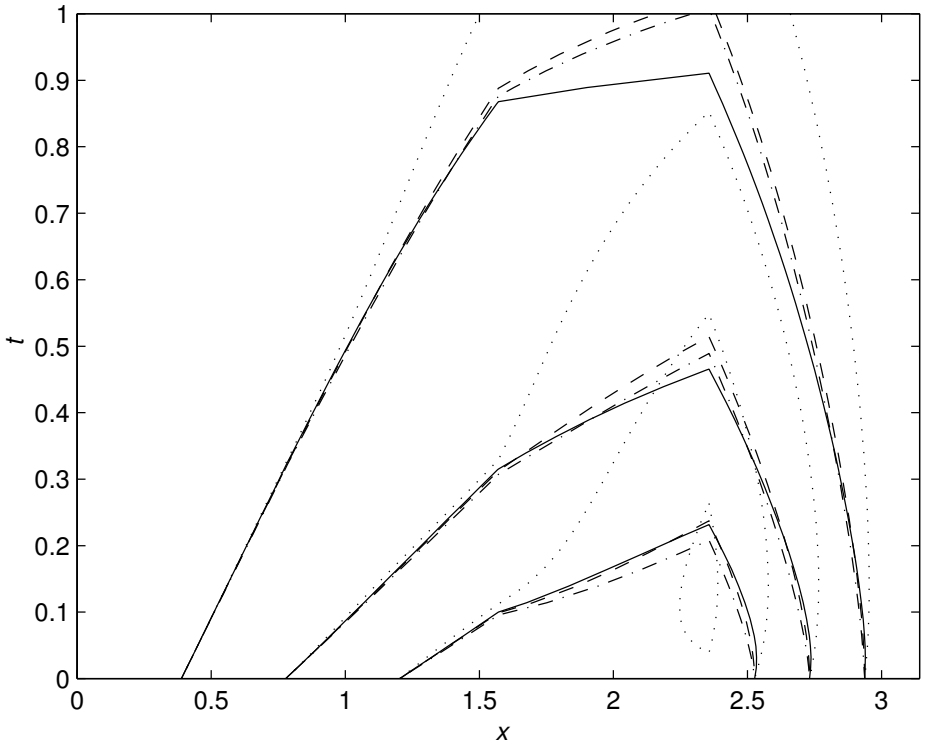


Figure 2: Contours of an exact solution $u(x,t)$, —, to compare with numerical models (18): \cdots , the conventional quadratically nonlinear approximation; $-\cdot-\cdot-$, the cubic approximation; $- - -$, the quintic approximation. Burgers' equation (1) with parameters $\alpha = 6$ and $\beta = 0$ is discretised on $m = 8$ elements in $[0, 2\pi)$ and drawn with contour interval $\Delta u = 0.2$.

Table 1: Comparison of the errors ε , defined in (19), of the spatially second order model (18) at the two first truncations in the nonlinearity, the $o(\alpha)$ quadratic and the $o(\alpha^2)$ cubic models, for various grid subintervals m . Observe that the higher order model is significantly less sensitive to the nonlinearity.

α	$m = 8$		$m = 16$		$m = 32$	
	$o(\alpha)$	$o(\alpha^2)$	$o(\alpha)$	$o(\alpha^2)$	$o(\alpha)$	$o(\alpha^2)$
1	.0116	.0095	.0031	.0025	.0008	.0006
3	.0356	.0109	.0102	.0040	.0026	.0011
6	.0694	.0115	.0215	.0059	.0054	.0018
10	.0971	.0186	.0318	.0055	.0081	.0026

$0 < t < 1$ with $m = 8$ and nonlinearity parameter $\alpha = 6$ are shown in Figure 2. Observe that the leading approximation (dotted) is significantly in error whereas the next two refinements (dot-dashed and dashed) are reasonably accurate (the closed dotted contour is caused by the leading approximation unphysically growing at its peak). The accuracy of the nonlinearly corrected models is remarkable considering the high level of nonlinearity, $\alpha = 6$, and the few points in the discretisation, $m = 8$.

For an assessment of errors over a range of parameters I record in Table 1 the overall error

$$\varepsilon = \max_t \left(\frac{1}{m} \sum_j |\epsilon_j(t)| \right), \tag{19}$$

where $\epsilon_j(t)$ is the difference between an approximation and the exact solution at the j th grid point. Observe the usual properties that the errors decrease with increasing spatial resolution m , and that the errors increase with increasing nonlinearity α . Our interest lies more in the comparison between the quadratic $o(\alpha)$ and cubic $o(\alpha^2)$ models (here the quintic $o(\alpha^4)$ model is virtually indistinguishable from the cubic

model). For small nonlinearity, $\alpha = 1$, there is very little difference; presumably the errors are dominated by the second-order approximation of spatial derivatives. As the nonlinearity α increases, the error of the quadratic approximation increases roughly in proportion to α , but the error of the cubic approximation grows much more slowly. We conclude, as centre manifold theory assures us, that the nonlinearly corrected cubic model more accurately captures the nonlinear dynamics of Burgers' equation.

4 Higher order approximations are more accurate

So far I have reported results only to first order in the coupling coefficient γ . Retaining higher orders in γ gives higher order difference rules as the coupling between adjacent elements is always ameliorated by a power of γ . However, it is only with the specific coupling of (8) that the $2p + 1$ width stencil, obtained by retaining terms in γ^p , attains $2p$ th-order accuracy in the linear terms. Retaining γ^2 terms, for example, then gives a fourth-order model which also performs remarkably well, especially for larger nonlinearities.

The particular form of the artificial internal boundary condition (8) controls the flow of information between elements of the discretisation. When $\gamma = 1$ the condition reduces to requiring the desired continuity: $u^- = u^+$ from the rightmost term and $u_x^- = u_x^+$ from (7) where, as before, the superscripts \pm denote evaluation at the internal boundary of expressions from the right/left-hand elements respectively. But we have enormous freedom in choosing the $(1 - \gamma)$ -term in (8). Our first requirement is that when $\gamma = 0$ it insulates the elements from each other so that the values of u_j in each element are independent in the centre manifold analysis. This is achieved in conjunction with (7) by only involving $u_x^- + u_x^+$ and its time derivatives. This is all that is necessary

to apply centre manifold theory.

However, computer algebra experiments show that generally we have to sum to high-order in γ to recover standard finite difference formulae for the linear diffusion term u_{xx} . This is impractical because the width of the finite difference formula grows linearly with the order of γ , although in Appendix A I show high order convergence to a global discretisation of periodic solutions. But we have freedom to find an interaction which recovers the standard formulae for the linear terms at low-orders in γ . Computer algebra experiments show that the expansion (9) for \mathcal{A} ensures the linear diffusion term is modelled with errors $\mathcal{O}(h^{2p})$ by a $2p + 1$ width finite difference stencil when the centre manifold is constructed with errors $\mathcal{O}(\gamma^{p+1})$, for $p = 1, \dots, 4$. The expression for \mathcal{A} in (9) is recognised to be the “asymptotic expansion” of the operator

$$\mathcal{A} = \frac{2}{h\sqrt{\partial_t}} \tanh\left(h\sqrt{\partial_t}/2\right).$$

The reason for the desirability of this particular operator may lie via the following observation. In the linear dynamics, $u_t = u_{xx}$ and so effectively $\partial_t = \partial_x^2$. Denoting the fundamental spatial differential operator by $\mathcal{D} = h\partial_x$, observe that in effect

$$\mathcal{A} = \frac{2}{\mathcal{D}} \tanh(\mathcal{D}/2) = \frac{\delta}{\mathcal{D}\mu},$$

where δ denotes the centred difference and μ the centred averaging operators:

$$\delta u_j = u_{j+1/2} - u_{j-1/2}, \quad \mu u_j = \frac{1}{2} (u_{j+1/2} + u_{j-1/2}).$$

Using this in (9), “cancelling” \mathcal{D} and “multiplying” by μ leads to the internal boundary condition being equivalent to

$$(1 - \gamma)\delta\frac{1}{2}(u^+ + u^-) = \gamma\mu(u^+ - u^-). \quad (20)$$

This has a pleasing symmetry as $(u^+ + u^-)/2$ on the left is like the averaging operator μ on the right, and the $(u^+ - u^-)$ on the right is like the differencing operator δ on the left. Further research on this form of the internal boundary conditions drafted in [39] shows that this discrete form quite generally ensures consistency for the linear terms as the grid spacing $h \rightarrow 0$.

Approximations to fourth order accuracy in space will be explored to verify their accuracy. Fourth order approximation formulae are obtained by truncating the analysis to errors $\mathcal{O}(\gamma^3)$. This enables the direct interaction between neighbouring elements through the $\mathcal{O}(\gamma)$ terms and the indirect interaction with the next nearest neighbours through $\mathcal{O}(\gamma^2)$ terms. Running the computer algebra program listed in Appendix B to higher order in γ gives the following for the evolution of the amplitudes u_j (using the centred difference and averaging operators δ and μ for compactness):

$$\begin{aligned}
 \dot{u}_j = & \frac{\gamma}{h^2} \delta^2 u_j - \frac{\gamma \alpha}{h} u_j \mu \delta u_j - \beta u_j^3 + \gamma \left[\frac{\alpha^2}{12} u_j^2 \delta^2 u_j - \frac{\beta}{24} (3 u_j^2 \delta^2 u_j + \delta^2 u_j^3) \right] \\
 & + \gamma^2 \left[\frac{1}{12 h^2} \delta^4 u_j \right. \\
 & + \frac{\alpha}{48 h} (2 \mu \delta (u_j \delta^2 u_j) + 24 u_j \mu^3 \delta u_j - 10 \mu \delta u_j^2 - 4 u_j \mu \delta u_j) \\
 & + \frac{\alpha^2}{24} (u_j \delta^2 u_j^2 - 4 u_j^2 \delta^2 u_j) + \frac{\alpha^2}{5760} (5 \delta^2 (u_j^2 \delta^2 u_j) - 69 u_j^2 \delta^4 u_j \\
 & - 120 u_j \delta^2 (u_j \delta^2 u_j) - 58 u_j (\delta^2 u_j)^2) \\
 & + \frac{\beta}{8} (\delta^2 u_j^3 - 2 u_j \delta^2 u_j^2 + 3 u_j^2 \delta^2 u_j) + \frac{\beta}{1440} (-\delta^4 u_j^3 \\
 & + 87 \delta^2 (u_j^2 \delta^2 u_j) + 87 u_j (\delta^2 u_j)^2 + 18 u_j^2 \delta^4 u_j) \left. \right] \\
 & + \mathcal{O}(\|u\|^4, \gamma^3).
 \end{aligned} \tag{21}$$

The first line give terms from the model discussed in the previous section, but here shown to lower order in $\|u\|$. The second line gives the ap-

Table 2: Comparison of the errors ε , defined in (19), of the spatially fourth order model (21) truncated to quadratic terms, $o(\alpha)$, and to quartic terms, $o(\alpha^3)$, for various grid subintervals m . Observe that the quartic model is significantly less sensitive to the nonlinearity.

α	$m = 8$		$m = 16$	
	$o(\alpha)$	$o(\alpha^3)$	$o(\alpha)$	$o(\alpha^3)$
1	.0013	.0016	.0003	.0003
3	.0070	.0090	.0009	.0021
6	.0252	.0131	.0020	.0052
10	.0464	.0132	.0066	.0066
20	.0659	.0171	.0179	.0056
30	.0683	.0196	.0250	.0061

propriate correction for the linear diffusion term u_{xx} to make it fourth order accurate in space. The third line gives a cubic, fourth order correction for the advection terms αuu_x . The fourth and further lines give spatially fourth order corrections to the higher order nonlinear terms.

These fourth order in space terms ensure a higher accuracy. Setting the artificial parameter $\gamma = 1$ and truncating at various orders in $\|u\|$, equivalently in α upon setting $\beta = 0$ as before, I find that to see any appreciable difference between the nonlinearly higher-order models we have to increase the nonlinear parameter to $\alpha = 10$ or more (from $\alpha = 6$ used in the previous section). See in Figure 3 that the nonlinearly low-order approximation is a little in error, but that the higher-order models are generally better. They are reasonably accurate despite the large nonlinearity, $\alpha = 10$, even though there is only $m = 8$ intervals in one period. A more comprehensive summary of the numerical errors is given in Table 2 which compares the overall error ε , see (19), for $m = 8$ and $m = 16$ elements over one period for the nonlinearity parameter ranging over $1 \leq \alpha \leq 30$. Once again observe that the conventional quadratic model has errors roughly proportional

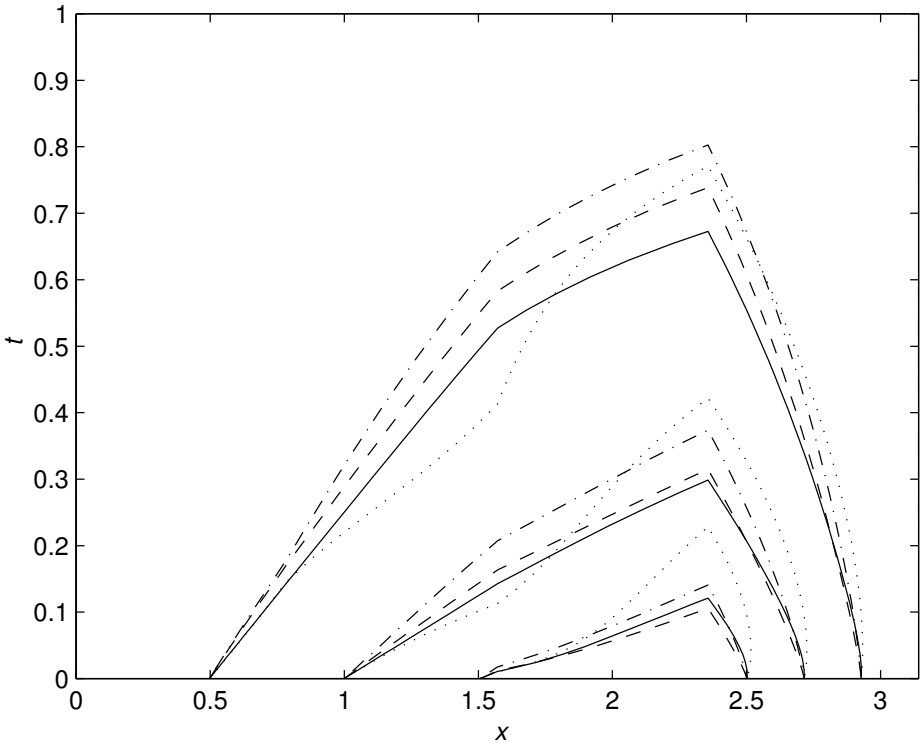


Figure 3: Contours of exact solution $u(x, t)$, —, to compare with fourth order numerical approximations (21): $\cdot \cdot \cdot$, the conventional quadratically nonlinear approximation; $-\cdot-\cdot-$, the cubic model; and $- - -$, the quartic model. Burgers' equation (1) with parameters $\alpha = 10$ and $\beta = 0$ is discretised on $m = 8$ intervals and drawn with contour interval $\Delta u = 0.2$.

to α , whereas the quartic model is much less sensitive. As the model is fourth order in space the errors here are an order of magnitude smaller than those in Table 1 of the previous section. This confirms the effectiveness of this approach to developing finite difference models.

However, because of the subtleties in the analysis of the nonlinear terms, the equivalent partial differential equation of a derived finite difference model will not reduce to the original PDE to the expected order in h . For example, here the equivalent PDE of the model (21), with $\gamma = 1$, is

$$\frac{\partial u}{\partial t} + \alpha u \frac{\partial u}{\partial x} = \frac{\partial^2 u}{\partial x^2} - \beta u^3 + \frac{h^2}{12} \left(-2\alpha u_x u_{xx} + \alpha^2 u u_x^2 \right) + \mathcal{O}(h^4), \quad (22)$$

which apparently differs from the generalised Burgers' equation by $\mathcal{O}(h^2)$. But note that this equivalent differential equation is obtained as $h \rightarrow 0$ keeping $\|u\|$ fixed, whereas the centre manifold model (21) is derived for fixed h as $\|u\| \rightarrow 0$ but taking full account of nonlinear dynamics within the domain. The numerical results presented here support my contention that this centre manifold approach better models the PDE for finite h and $\|u\|$.¹

5 Nonlinear stability of the discretisations

In this section I explore a little the stability of the discretisations for the modified Burgers' equations (1). Most discretisation schemes are reliable for the low wavenumber, large scale structures. Unphysical instabilities generally occur for high wavenumber, small scale structures because for these modes the finite differences are inaccurate estimates

¹It is conceivable that a more carefully crafted interaction between the elements, modifying (8), may achieve $\mathcal{O}(h^{2p})$ consistency between the finite difference model and *all* terms of the original PDE when constructing such a centre manifold model to $\mathcal{O}(\gamma^{p+1}, \|u\|^q)$.

of the spatial derivatives. Thus, following Fornberg [13] and Foias et al. [10], I here investigate the nonlinear dynamics of high wavenumber modes in various discretisations. The analysis is done on a case by case basis. Low order models have a simple structure in which global stability is easily seen. However, higher order models have a more intricate structure for which stability is harder to achieve.

First consider the cubic nonlinear models, errors $\mathcal{O}(\|u\|^4)$, for the various orders of spatial discretisation. The model which is second order accurate in space, that is neglecting terms $\mathcal{O}(\gamma)$, was examined in the Introduction. There we reaffirmed that for the conventional quadratic model, the advection generates instabilities (4). This conclusion is based upon analysing the dynamics of the modes

$$u_j = \sigma(t) \frac{1}{h\sqrt{3}} \sin(\pi j/3) + \zeta(t) \frac{1}{h\sqrt{3}} \sin(2\pi j/3) + \eta(t) \frac{1}{h} \cos(\pi j), \quad (23)$$

although the sawtooth mode $\cos(\pi j)$ was not included in the Introduction. A similar analysis of the cubic model gave (5–6) which show that the modes are nonlinearly stable if $\beta \geq -\alpha^2/10$; for β more negative than this, the nonlinear reaction term $-\beta u^3$ can overcome dissipation to cause σ to blow-up in finite time from sufficiently large initial conditions—of course this is qualitatively correct for nonlinear reaction ($\beta < 0$). However, the stability for $\beta \geq -\alpha^2/10$ is only assured for the particular modes in (23) which have a wavenumber of one third and two thirds of the maximum resolvable by the grid. To cover a wider range of wavenumbers we also investigate the highest wavenumber mode, $u_j = \eta(t) \frac{1}{h} \cos(\pi j)$ as included in (23). I find that this sawtooth mode is stable for both of these models: $\dot{\eta} = -4\eta$ for the quadratic model; whereas for the cubic model $\dot{\eta} = -4\eta - \frac{1}{3}(\beta + \alpha^2)\eta^3$ which is nonlinearly stable provided $\beta \geq -\alpha^2$. Thus the cubic, second order model, errors $\mathcal{O}(\gamma^2, \|u\|^4)$, is nonlinearly stable provided the nonlinear reaction is not too strong (negative β).

This stability comes from the $\alpha^2/12 u_j^2 \delta^2 u_j$ term in (3) or (17) which could either be interpreted as an upwind difference modification, or as

a nonlinear enhancement to diffusion. Combining it with the advection term $-\alpha/h u_j \mu \delta u_j$ leads to

$$\begin{aligned} -\frac{\alpha}{h} u_j \mu \delta u_j + \frac{\alpha^2}{12} u_j^2 \delta^2 u_j &= -\frac{\alpha}{h} u_j \left[\mu \delta u_j - \frac{\alpha h}{12} u_j \delta^2 u_j \right] \\ &\approx -\alpha u(x_j) u_x(x_j - \alpha h u_j / 12). \end{aligned}$$

Thus one interpretation of the nonlinear correction is to approximately evaluate the derivative a distance $\alpha h u_j / 12$ upwind of the grid point x_j . Another, even simpler, interpretation follows by combining it with the diffusion term $\frac{1}{h^2} \delta^2 u_j$ whence

$$\frac{1}{h^2} \delta^2 u_j + \frac{\alpha^2}{12} u_j^2 \delta^2 u_j = \left(1 + \alpha^2 h^2 u_j^2 / 12\right) \frac{1}{h^2} \delta^2 u_j \approx \left(1 + \alpha^2 h^2 u^2 / 12\right) u_{xx}.$$

This indicates that the nonlinear advection, flagged by the coefficient α , may interact with diffusion within an element to increase the dissipation. Either of these interpretations are effects known to often enhance stability. Recent research on the linear advection-diffusion equation [39] shows that the holistic finite difference model is stable for *all* advection speeds and grid spacing.

The model of Burgers' equation which is quadratic in the nonlinearity but fourth order in spatial discretisation is obtained by truncating (21) to errors $\mathcal{O}(\gamma^3, \|u\|^3)$ (omit all terms involving β and α^2). Substituting the modes (23), deduce the equations for the amplitudes to be

$$\begin{aligned} h^2 \dot{\sigma} &= -\frac{13}{12} \sigma + \frac{\alpha}{12} \sigma \zeta, \\ h^2 \dot{\zeta} &= -\frac{15}{4} \zeta + \frac{3\alpha}{8} \zeta^2 - \frac{7\alpha}{24} \sigma^2, \\ h^2 \dot{\eta} &= -\frac{16}{3} \eta. \end{aligned}$$

Clearly the sawtooth mode decays, but expect the other two modes to be nonlinearly unstable because of the presence of three fixed points at

finite amplitudes in σ and ζ . However, computing the first nontrivial correction to the centre manifold, the cubic model, gives the approximate model (21), and then the evolution of the modes (23) are

$$\begin{aligned} h^2 \dot{\sigma} &= -\frac{13}{12}\sigma + \frac{\alpha}{12}\sigma\zeta + \sigma\zeta^2 \left(-\frac{809}{1920}\beta - \frac{2513}{11520}\alpha^2 \right) \\ &\quad + \sigma^3 \left(-\frac{1369}{5760}\beta - \frac{181}{11520}\alpha^2 \right), \\ h^2 \dot{\zeta} &= -\frac{15}{4}\zeta + \frac{3\alpha}{8}\zeta^2 - \frac{7\alpha}{24}\sigma^2 + \zeta^3 \left(-\frac{89}{640}\beta - \frac{141}{1280}\alpha^2 \right) \\ &\quad + \sigma^2\zeta \left(-\frac{173}{384}\beta - \frac{277}{2304}\alpha^2 \right), \\ h^2 \dot{\eta} &= -\frac{16}{3}\eta + \eta^3 \left(-\frac{19}{90}\beta - \frac{121}{180}\alpha^2 \right). \end{aligned}$$

Clearly, from the last equation, the sawtooth mode is always stable unless the reaction is very strong. Also clearly the nonlinear damping ($\beta > 0$) always acts to stabilise the other two modes unless it becomes a sufficiently strong reaction ($\beta < 0$). The σ equation, apart from $\sigma = 0$, has no zeros for $\beta \geq -\alpha^2 181/2738$ and hence $\sigma \rightarrow 0$ for this range of β . For this range of β and setting $\sigma = 0$, the ζ equation has no zeros apart from $\zeta = 0$, thus $\zeta \rightarrow 0$. This fourth order model is nonlinearly stable.

However, a similar analysis of the sixth and eighth order cubic models shows that they are nonlinearly unstable for sufficiently large initial conditions. For example, the sawtooth mode in the sixth order model is unstable for $|\eta| > \frac{4}{\alpha} \sqrt{\frac{238}{15}}$ when $\beta = 0$, that is, for u_j more extreme than about $(-1)^j 16/(h\alpha)$. Thus, although the nonlinear centre manifold analysis does appear to improve stability, it may not be enough for extreme initial conditions.

The second set of models to consider are those of higher order in the nonlinearity. The next simplest is the quartic, second order model

obtained by truncating (17). This model includes the terms involving interactions between the advection and reaction nonlinearities, flagged by $\alpha\beta$ in the coefficient. I find the sawtooth mode is stable. The dynamics of σ and ζ are more involved: numerically I observe that large solutions may grow for a while but that they generically get reinjected into the stable domain surrounding the origin. This model is almost always nonlinearly stable. Unfortunately, including the next order of nonlinearity gives model (17) which numerically is seen to be unstable for initial conditions any larger than roughly $|\sigma| + |\zeta| \approx 15/\alpha$. However, investigating the quintic, fourth order model, I find it is nonlinearly stable for small reaction β , though for larger β , large enough initial conditions may blow up.

My conclusions for this section are: the nonlinear centre manifold analysis often improves stability; but, as is typical for Taylor series based on small amplitude asymptotics, the qualitative results of evaluation at large amplitude depends sensitively upon the truncation.

6 Simplify models with a coordinate transform

So far we have maintained precisely, through the condition (15), the definition of the parameters of the model, namely that u_j are the values of the field u at the grid points, $u_j = u(x_j, t)$. We have the opportunity to simplify the model by a nonlinear, near identity reparametrisation of the centre manifold—such transforms also lie behind the classification of bifurcations by their normal form [18, e.g.]. For example, here we may relax (15) and seek solutions for which

$$u(x_j, t) = u_j + Bu_j^2 + \mathcal{O}(u_j^3), \quad (24)$$

for some coefficient B which we are free to chose. Then u_j no longer is precisely the value of u at the grid point x_j , but some other, though

nearly the same, measure of the local amplitude of the solution field $u(x)$. A quick computation then shows that the resultant quadratic model would be this modified version:

$$\ddot{u}_j = \frac{\gamma}{h^2} \delta^2 u_j - \frac{\alpha\gamma}{h} u_j \mu \delta u_j + \frac{B\gamma}{h^2} [\delta^2(u_j^2) - 2u_j \delta^2 u_j] + \mathcal{O}(\gamma^2, \|u\|^3). \quad (25)$$

Upon expanding the centred differences, the transformation introduces five quadratic terms which may be used to simplify the model. Here either one of the advection terms in $u_j \mu \delta u_j$ can be eliminated by choosing $B = \pm \alpha h/4$, but only at the cost of introducing three new terms. Thus the unique best choice is to set $B = 0$ in order to minimise the number of terms in the model. In this section we briefly look at the few algebraic simplifications that ensue at higher orders through using such near identity coordinate transforms.

Most previous work on inertial manifolds has used the amplitudes of the eigenfunctions to parametrise the inertial manifold [9, e.g.]. However, Foias & Titi [12] considered two different parametrisations: the grid values (as we have used so far); and the element average values. In their analysis of the Kuramoto-Sivashinsky equation Foias & Titi suggest that the latter parametrisation is significantly more effective: compare their Theorem 3.2 with their Theorem 3.1. But the theorems only address the existence of a parametrisation of the inertial manifold, not the accuracy nor the stability. At this stage there seems no a priori reason for knowing if any one parametrisation is better than any other. Simplifying the algebraic form of the model at least reduces the amount of computation and so is the aim of this section.

First see that the near identity coordinate transform should only involve u_j . In general the transform may be of the form

$$u(x_j, t) = u_j + f(u_j, u_{j\pm 1}, u_{j\pm 2}, \dots), \quad (26)$$

where f is some strictly nonlinear function to be chosen. But consider what happens if we construct a model to error $\mathcal{O}(\gamma^{p+1})$, that is, we ac-

count for p interactions between neighbouring elements. If the coordinate transform f depends upon u_{j+k} then the p interactions will generate terms in the centre manifold and the evolution thereon involving $u_{j+k\pm p}$. Thus the coordinate transform will generate new terms outside the range of width $2p + 1$ in the normal model, u_{j-p}, \dots, u_{j+p} . The only way to avoid these extra terms appears to be by avoiding the inclusion of $u_{j\pm k}$, $k \neq 0$, in the transform (26). Thus we restrict attention to near identity transforms of the very much simpler form

$$u(x_j, t) = u_j + f(u_j). \quad (27)$$

It is quite straightforward to investigate the possible coordinate transforms in particular examples using computer algebra. In the computer algebra program in Appendix B, for example, to try the transformation with $f(u_j) = Bu_j^2 + Cu_j^3$ we just change line 40, that gives the initial approximation, to

```
v:=usz*u(j)+usz^2*bb*u(j)^2+usz^3*cc*u(j)^3;
```

and seek values of **bb** and **cc** to simplify the model. this works because all corrections v' to the centre manifold are found such that $v'(x_j) = 0$, hence we maintain throughout the amplitude equation that $u(x_j) = u_j + Bu_j^2 + Cu_j^3$. In this problem, we find setting $B = 0$ not only simplifies the quadratic terms in the model, it also eliminates two $u_j u_{j\pm 1}^2$ terms at $\mathcal{O}(\|u\|^3)$. Then two choices are apparent for C :

- setting $C = h^2\beta/24$ eliminates $u_{j\pm 1}^3$ terms to give the model

$$\begin{aligned} \dot{u}_j = & \frac{\gamma}{h^2} \left(1 + \frac{\alpha^2 h^2 u_j^2}{12} \right) \delta^2 u_j - \frac{\gamma \alpha}{h} u_j \mu \delta u_j - \beta u_j^2 \left(1 + \frac{\gamma \delta^2}{4} \right) u_j \\ & + \mathcal{O}(\|u\|^4, \gamma^2), \end{aligned}$$

which only changes (3) in the cubic reaction term;

- whereas setting $C = h^2(2\alpha^2 - 3\beta)/72$ eliminates $u_j^2 u_{j\pm 1}$ terms from (3) to give

$$\begin{aligned} \dot{u}_j = & \frac{\gamma}{h^2} \delta^2 u_j - \frac{\gamma \alpha}{h} u_j \mu \delta u_j + \frac{\gamma \alpha^2}{36} \delta^2 u_j^3 - \beta \left(1 + \frac{\gamma \delta^2}{12} \right) u_j^3 \\ & + \mathcal{O}(\|u\|^4, \gamma^2). \end{aligned}$$

At present there seems no reason to prefer one of these over the other. Calculating to the next order in $\|u\|$ indicates that it is best to have no quartic term in the transformation (27), and in particular such a quartic term cannot eliminate the terms representing the interactions between the different nonlinearities that are identified in (17). Apparently, these nonlinear coordinate transforms can only simplify a little the algebraic form of the model.

Unexplored possibilities are to use these coordinate transforms to either simplify in some way the actual shape of the centre manifold, rather than the model, or perhaps more usefully to ensure there is no unphysical nonlinear stability in the model. For example, following the analysis of §5, by choosing $C \leq -249\alpha^2 h^2 / 44128$ we globally stabilise the high wavenumber dynamics of the sixth order, cubic model.

7 Conclusion

Using centre manifold theory is a new approach to deriving finite difference models of dynamical systems. Many details need further research for general application of the theory. However, this particular example application to a generalised Burgers' equation (1) shows many promising features.

By introducing artificial internal boundaries we apply centre manifold theory (§2). The internal boundaries divide the domain of interest into sub-domains that look very much like finite elements. The theory

guarantees essential properties required for a low-dimensional model, though the need to evaluate the asymptotic expressions for $\gamma = 1$ weakens this assurance. First, a model exists parametrised in any reasonable way we desire. Second, the model is approached exponentially quickly by the original dynamics, in a time of $\mathcal{O}(h^2)$ for Burgers' equation, but possibly much quicker for higher-order PDEs. The same theorem also assures us that at least for small nonlinearities the numerical model shares the same stability as the original PDE dynamics. The stability at large nonlinearity is more problematical as discussed in §5. Lastly, an approximation to the model may be found to any order in the nonlinearity, using computer algebra for example. The resultant finite difference models are independent of valid rearrangements of the governing PDE. In effect this technique analyses the actual dynamics of the PDE as a whole—this is a holistic approach. For example, I am not aware of any other finite difference discretisation method that develops cross terms between the nonlinearities, though inertial manifolds generally couple all modes in their global approximations. Specific numerical simulations in §3 and §4 show that the finite difference models derived for Burgers' equation are indeed accurate.

Further research is needed to incorporate physical boundary conditions into the model. The extra analysis should be straightforward, but the level of detail would increase significantly as near the physical boundary we would lose the translational symmetry between the elements. Then the intriguing issue of initial conditions needs further work. Following [32, 8, 38] we note that to make accurate forecasts with the numerical models we need to provide initial values u_j^0 which are not the initial field $u_0(x)$ sampled at the collocation points x_j . Instead preliminary work shows that u_j^0 should be approximately the average of $u_0(x)$ over each element. Non-autonomous forcing of the PDE will need projecting onto the finite difference grid in a similar manner. The analysis of other PDEs in possibly higher-spatial dimensions would appear to hinge upon being able to solve the linear part of the PDE over the elements subject to forcing from the coupling across the artificially

introduced internal boundaries. This is potentially quite complicated, but the results of the simple problems here suggest that the analysis could be very worthwhile.

Acknowledgements: this work was supported by a grant from the Australian Research Council. I thank some referees for prompting useful revisions to this paper.

A Global discretisations converge to spectral accuracy

In this work so far I have striven to make the discretisation to have as small a width stencil as possible. As discussed in §4, I have done this by requiring that the interaction between adjacent elements, which we are moderately free to choose, be immediately consistent with traditional finite difference formula for the spatial derivatives. In this short section we abandon the need for a small width and instead seek a global model of periodic solutions to Burgers' equation to compare in spirit with Foias & Titi's [12] discrete reparametrisation of their global inertial manifolds of the Kuramoto-Sivashinsky equation. This appendix is not intended to provide a good method of constructing such global inertial manifolds, but merely to illuminate the connection between this and other approaches. We will see empirical evidence that the asymptotic expansion in the parameter γ appears to converge for $\gamma = 1$ to a spectral approximation for at least this particular problem.

Foias & Titi [12] proved that a model, their so-called inertial form (3.6), exists in the form of a parametrisation in terms of values of u at discrete points. Their arguments are based on the spectral representation of the inertial manifolds and in essence just proves the existence

of a coordinate transformation between the two forms, albeit nonlinear. However, their example explicit discretisation (4.7) has no guarantees from their theory as it is entirely based upon the usual finite difference approximation; they write [12, p146,(ii)] “the finite difference scheme (4.7) provides a good approximation to the *qualitative* dynamics” (my italics). In contrast, I provide here a construction that is rigorous in a neighbourhood of $\gamma = 0$ and converges up to the problem of interest $\gamma = 1$. Even though more investigation needs to be done on the properties at $\gamma = 1$, the model and the rigorous theory are here derived from the same base. This construction is an alternative to that which might have been done from a spectral representation, but it should converge to the same model even though the theoretical basis is different.

To derive a global model of Burgers equation (1) here is a simple matter. Somewhat arbitrarily, let us choose to model periodic solutions on a finite domain of length say 2π with m equi-spaced grid points so that $h = 2\pi/m$. The parameters of the model are then u_0, \dots, u_{m-1} . The periodicity is built in to the analysis simply by setting any reference to u_j outside these variables to $u_{j \pm m}$ among the variables. Lastly, the interaction operator \mathcal{A} appearing in (8) is replaced by the constant 1²—in this section we have no need to reproduce at low order traditional finite difference formula. Then the modified version of the computer algebra programme in Appendix B is run to relatively high orders in γ .

For example, look at the case of $m = 4$ grid points in one period. For simplicity I only investigate Burgers’ equation and so set $\beta = 0$. To low order in the interaction γ the model is found to be

$$\frac{du_j}{dt} = \frac{1}{h^2} \left[u_{j-1} \left(\frac{2}{3}\gamma^2 + \gamma \right) - \frac{1}{3}u_{j+2}\gamma^2 + u_{j+1} \left(\frac{2}{3}\gamma^2 + \gamma \right) + u_j \left(-\gamma^2 - 2\gamma \right) \right]$$

²The constant \mathcal{A} could take the role of an Euler parameter [1, Chapt. 8] in seeking transformations of a power series in order to improve convergence, but this is not attempted here.

Table 3: coefficients in the high order expansion in γ of some terms in the global model (28) showing convergence to a spectrally accurate model.

	u_j	$u_{j\pm 1}$	u_{j+2}	$\mp u_{j\pm 1}^2$	$\mp u_j u_{j\pm 1}$	$u_{j+1} u_{j-1} u_{j+2}$
γ	-0.8106	0.4053	0	0	0.3183	0
γ^2	-0.4053	0.2702	-0.1351	0.0928	0.0663	0
γ^3	-0.1801	0.1711	-0.1621	0.1149	-0.0615	0.0109
γ^4	-0.0733	0.1012	-0.1291	0.0963	-0.0986	0.0452
γ^5	-0.0309	0.0541	-0.0772	0.0625	-0.0815	0.0801
γ^6	-0.0159	0.0240	-0.0321	0.0299	-0.0433	0.0912
γ^7	-0.0086	0.0062	-0.0039	0.0063	-0.0079	0.0722
γ^8	-0.0023	-0.0031	0.0084	-0.0070	0.0128	0.0363
γ^9	0.0033	-0.0070	0.0106	-0.0117	0.0178	0.0040
γ^{10}	0.0068	-0.0076	0.0084	-0.0104	0.0125	-0.0109
γ^{11}	0.0076	-0.0066	0.0057	-0.0062	0.0039	-0.0073
γ^{12}	0.0062	-0.0049	0.0037	-0.0014	-0.0028	0.0059
\sum	-1.5030	1.0029	-0.5027	0.3660	0.1360	0.3275

$$\begin{aligned}
& + \frac{\alpha}{h} \left[\frac{7}{48} u_{j-1}^2 \gamma^2 - \frac{1}{16} u_{j-1} u_{j+2} \gamma^2 + u_{j-1} u_j \left(\frac{5}{48} \gamma^2 + \frac{1}{2} \gamma \right) \right. \\
& \quad \left. + \frac{1}{16} u_{j+2} u_{j+1} \gamma^2 - \frac{7}{48} u_{j+1}^2 \gamma^2 + u_{j+1} u_j \left(-\frac{5}{48} \gamma^2 - \frac{1}{2} \gamma \right) \right] \\
& + \alpha^2 \left[\frac{7}{576} u_{j-1}^3 \gamma^2 - \frac{7}{1152} u_{j-1}^2 u_{j+2} \gamma^2 + \frac{43}{640} u_{j-1}^2 u_j \gamma^2 \right. \\
& \quad - \frac{1}{24} u_{j-1} u_{j+2} u_j \gamma^2 - \frac{29}{1440} u_{j-1} u_{j+1} u_j \gamma^2 \\
& \quad + u_{j-1} u_j^2 \left(\frac{1}{320} \gamma^2 + \frac{1}{12} \gamma \right) - \frac{7}{1152} u_{j+2} u_{j+1}^2 \gamma^2 - \frac{1}{24} u_{j+2} u_{j+1} u_j \gamma^2 \\
& \quad \left. - \frac{109}{2880} u_{j+2} u_j^2 \gamma^2 + \frac{7}{576} u_{j+1}^3 \gamma^2 + \frac{43}{640} u_{j+1}^2 u_j \gamma^2 \right]
\end{aligned}$$

$$\begin{aligned}
& + u_{j+1}u_j^2 \left(\frac{1}{320}\gamma^2 + \frac{1}{12}\gamma \right) + u_j^3 \left(-\frac{11}{960}\gamma^2 - \frac{1}{6}\gamma \right) \\
& + \mathcal{O}(\gamma^3, \|u\|^4).
\end{aligned} \tag{28}$$

We seek to evaluate this sort of model for $\gamma = 1$ in order to obtain the various coefficients in the model. However, it is clear that we need to compute higher orders in γ in order to obtain accurate coefficients. Some results of such a high order expansion are shown in Table 3. It is not clear that the expansions converge at $\gamma = 1$ especially for the cubic nonlinear term shown; however, after computing the linear terms alone to $\mathcal{O}(\gamma^{30})$ and drawing in Figure 4 a generalised Domb-Sykes plot [26, Appendix] it is evident that the radius of convergence in γ is $R \approx 1.25$. Moreover, the coefficients of the linear terms sum to within one percent of the correct coefficients (of $-3/2$, 1 and $-1/2$) for spectral differentiation with four points in a period.

To show that the necessary continuity in the solution field u is approximately established at $\gamma = 1$ I plot in Figure 5 the centre manifold for the four shown points u_j ; see that the field u within each element very nearly joins smoothly to the next. Summing the terms at $\gamma = 1$ and recognising the cubic nonlinearities are more uncertain the model is then

$$\begin{aligned}
\frac{du_j}{dt} = & 1.003u_{j-1} - 0.503u_{j+2} + 1.003u_{j+1} - 1.503u_j \\
& + \alpha \left[0.366u_{j-1}^2 - 0.363u_{j-1}u_{j+2} + 0.136u_{j-1}u_j \right. \\
& \quad \left. + 0.363u_{j+2}u_{j+1} - 0.366u_{j+1}^2 - 0.136u_{j+1}u_j \right] \\
& + \alpha^2 \left[0.272u_{j-1}^3 - 0.0543u_{j-1}^2u_{j+2} + 0.326u_{j-1}^2u_{j+1} \right. \\
& \quad - 0.0163u_{j-1}^2u_j - 0.159u_{j-1}u_{j+2}^2 + 0.328u_{j-1}u_{j+2}u_{j+1} \\
& \quad - 0.205u_{j-1}u_{j+2}u_j + 0.326u_{j-1}u_{j+1}^2 - 0.00759u_{j-1}u_{j+1}u_j \\
& \quad - 0.168u_{j-1}u_j^2 - 0.107u_{j+2}^3 - 0.159u_{j+2}^2u_{j+1} - 0.149u_{j+2}^2u_j \\
& \quad \left. - 0.0543u_{j+2}u_{j+1}^2 - 0.205u_{j+2}u_{j+1}u_j - 0.0195u_{j+2}u_j^2 \right]
\end{aligned}$$

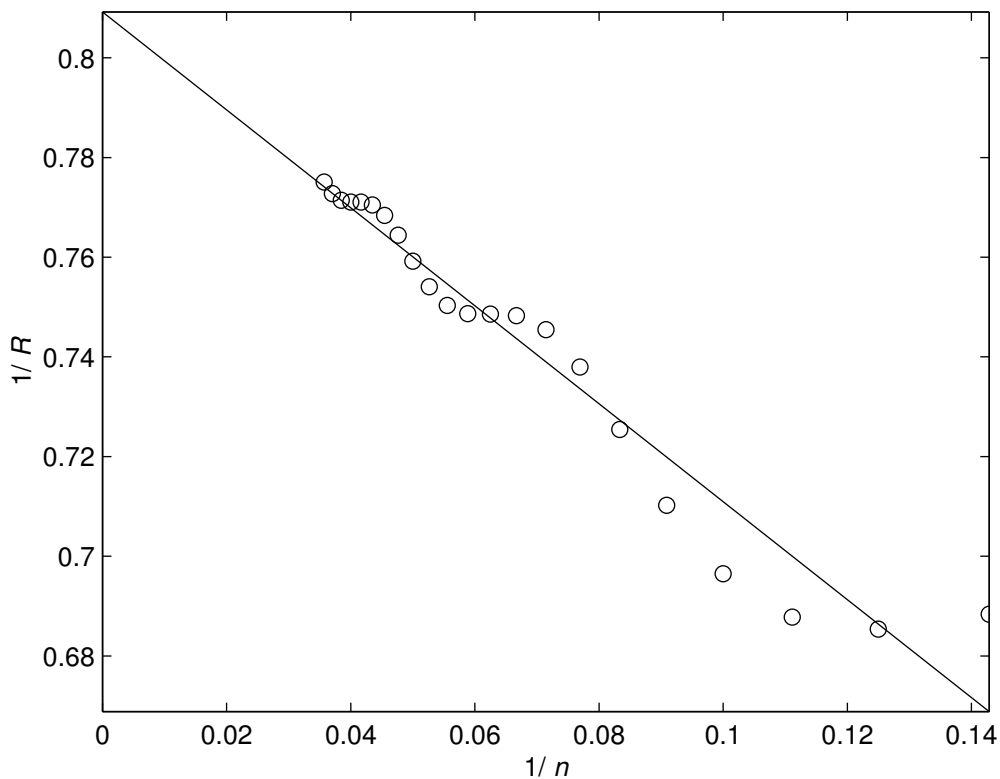


Figure 4: generalised Domb-Sykes plot for the expansion in γ to $\mathcal{O}(\gamma^{30})$ of the coefficient of the linear term $u_{j\pm 1}$ in the model (28). The linear extrapolation of the data points to $1/n = 0$ indicates a radius of convergence such that $1/R \approx 0.81$.

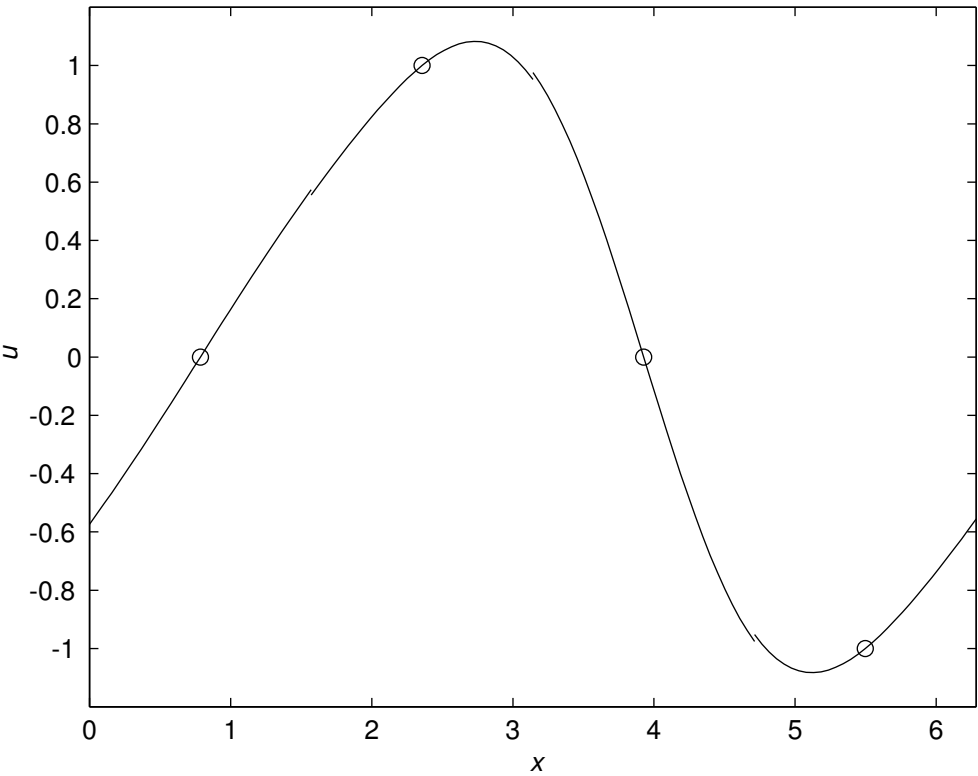


Figure 5: the centre manifold field $u(x)$ for the cubic nonlinear model with $\alpha = 0.8$, evaluated from a grid of four points, the circles, as obtained from the $\mathcal{O}(\gamma^{13})$ approximation used to generate Table 3. See how the predicted field u almost smoothly joins between the elements and how the peak is asymmetric due to the discretisation knowing about the advection within each element.

$$\begin{aligned}
& + 0.271u_{j+1}^3 - 0.0163u_{j+1}^2u_j - 0.168u_{j+1}u_j^2 - 0.0346u_j^3] \\
& + \mathcal{O}(\|u\|^4).
\end{aligned} \tag{29}$$

These asymptotics appear to converge to a spectrally accurate discretisation. Such global approximations to the dynamics are clearly very expensive to evaluate computationally (as also noted by García-Archilla et al. [17, 16])—just doubling the spatial resolution to $m = 8$ will increase the number of cubic terms in the model by a factor of about eight, and even more for higher order approximations. This is just one more reason that in the body of the article I have concentrated upon compact discretisations based upon a local analysis of the systems' dynamics.

B Computer algebra develops the approximations

Just one of the virtues of this centre manifold approach to modelling is that it is systematic. This enables relatively straightforward computer programs to be written to find the centre manifold and the evolution thereon [36, e.g.]. I believe computer algebra will be increasingly used to support research by performing extensive routine algebraic manipulations. To ensure correctness and to provide a basis for further work it seems reasonable to include the computer algebra code. Including the code here replaces extensive recording of elementary algebraic steps in the derivation of the results.

For this problem the iterative algorithm is implemented by a computer algebra program written in REDUCE³ Although there are many

³At the time of writing, information about `reduce` was available from Anthony C. Hearn, RAND, Santa Monica, CA 90407-2138, USA. <mailto:reduce@rand.org>

details in the program, the correctness of the results are *only determined* by driving to zero (line 59) the residual of the governing differential equation, evaluated on line 48, to the error specified on line 46 and with the residual of the internal boundary condition computed on lines 50–53. The other details only affect the rate of convergence to the ultimate answer.

```

COMMENT Try holistic finite differences on a generalised Burgers
1 equation. Consider ODEs of the form  $u_t - u_{xx} = f(u, u_x)$  for
2 strictly nonlinear  $f$  where for Burgers equation  $f \propto -u \cdot u_x$ 
3
4 Discretise the problem by mathematically introducing insulating
5 boundaries at grid midpoints, and coupling them together via a
6 parameter  $\gamma$  so that the original  $C^2$  holds at the midpoints
7  $\gamma=1$ . Treat  $\gamma$  as a perturbation parameter.
8
9 The unknown  $u(x,t)$  field is then a function of  $u_j(t)=u(x_j,t)$ , v
10 each  $u_j$  evolve according to  $du_j/dt=g_j$  .
11
12 Tony Roberts, 12 Sept 1998;
13
14 % improve printing
15 on div; off allfac; on revpri; factor gam,usz,h;
16
17 % make function of  $\xi=(x-x_j)/h$ 
18 depend xi,x;
19 let df(xi,x)=>1/h;
20
21 % parameterise with evolving  $u(j)$ 
22 operator u; depend u,t;
23 let df(u(~k),t)=>sub(j=k,g);
24
25 % intx computes  $\int_{-1/2}^{+1/2} \dots d\xi$ 
26 operator intx; linear intx;
27 let { intx(xi^~p,xi) => (1+(-1)^p)/(p+1)/2^(p+1)
28     , intx(xi,xi) => 0
29     , intx(1,xi) => 1 };
30

```

```

31 % solves v_xixi=RHS s.t. v(0)=0 and v_xi(+1/2)+v_xi(-1/2)=0
32 operator solv; linear solv;
33 let { solv(xi~~p,xi) => (xi^(p+2)/(p+2)-(1-(-1)^p)*xi/2^(p+2))/(p+2)
34       , solv(xi,xi) => (xi^3-3*xi/4)/6
35       , solv(1,xi) => (xi^2)/2 };
36
37 % linear solution in jth interval
38 % usz is used to measure the order of terms in u_j
39 v:=usz*u(j);
40 g:=0;
41
42 % iteration
43 % the BC is crafted s.t. gam^p kept gives (2p)th order in space
44 % by (1-gam)*delta(vp+v)h/2-gam*mu(vp-v)=0 recognising u_t=u_xx
45 let { gam^3=>0, usz^4=>0 } ;
46 repeat begin
47   deq:=df(v,t)-df(v,x,2)+(a*v*df(v,x)+b*v^3);
48   vp:=sub(j=j+1,v);
49   dv:=sub(xi=-1/2,vp)-sub(xi=1/2,v);
50   svd:=(h/2)*(sub(xi=-1/2,df(vp,x))+sub(xi=1/2,df(v,x)));
51   bcp:=(1-gam)*( svd -df(svd,t)*h^2/12 +df(svd,t,2)*h^4/120
52                -df(svd,t,3)*h^6*17/20160 ) -gam*( dv );
53   bcm:=sub(j=j-1,bcp);
54   gd:=(-bcp+bcm)/h^2-intx(deq,xi);
55   g:=g+gd/usz;
56   v:=v+h^2*solv(deq+gd,xi)-xi*(bcm+bcp)/2;
57   showtime;
58 end until (deq=0)and(bcp=0);
59 bcp:=sub(xi=-1/2,df(vp,x))-sub(xi=1/2,df(v,x)); % check other IB
60 deq:=sub(xi=0,v)-usz*u(j); % check amplitude
61
62 end;

```

References

- [1] C.M. Bender and S.A. Orszag. *Advanced mathematical methods for scientists and engineers*. McGraw-Hill, 1981. 37

- [2] J. Carr. *Applications of centre manifold theory*, volume 35 of *Applied Math. Sci.* Springer-Verlag, 1981. 4, 12
- [3] J. Carr and R.G. Muncaster. The application of centre manifold theory to amplitude expansions. I. ordinary differential equations. *J. Diff. Eqns.*, 50:260–279, 1983. 4
- [4] J. Carr and R.G. Muncaster. The application of centre manifold theory to amplitude expansions. II. Infinite dimensional problems. *J. Diff. Eqns.*, 50:280–288, 1983. 4, 14, 15
- [5] H.C. Chang. Onset of nonlinear waves on falling films. *Phys. Fluids A*, 1:1314–1327, 1989. 4
- [6] P. Constantin, C. Foias, B. Nicolaenko, and R. Temam. *Integral manifolds and inertial manifolds for dissipative partial differential equations*, volume 70 of *Applied Math. Sci.* Springer-Verlag, 1989. 15
- [7] S.M. Cox and A.J. Roberts. Centre manifolds of forced dynamical systems. *J. Austral. Math. Soc. B*, 32:401–436, 1991. 11
- [8] S.M. Cox and A.J. Roberts. Initial conditions for models of dynamical systems. *Physica D*, 85:126–141, 1995. 10, 35
- [9] C. Foias, M.S. Jolly, I.G. Kevrekedis, G.R. Sell, and E.S. Titi. On the computation of inertial manifolds. *Phys Lett. A*, 131:433–436, 1988. 8, 32
- [10] C. Foias, M.S. Jolly, I.G. Kevrekidis, and E.S. Titi. Dissipativity of numerical schemes. *Nonlinearity*, 4:591–613, 1991. 3, 4, 7, 28
- [11] C. Foias, G.R. Sell, and E.S. Titi. Exponential tracking and approximation of inertial manifolds for dissipative nonlinear equations. *J. Dyn. & Diff. Eqns.*, 1:199–244, 1989. 15

- [12] C. Foias and E.S. Titi. Determining nodes, finite difference schemes and inertial manifolds. *Nonlinearity*, 4:135–153, 1991. 3, 8, 9, 32, 36, 37
- [13] B. Fornberg. On the instability of the leap-frog and Crank-Nicolson approximations of a nonlinear partial differential equation. *Maths of Comput.*, 27:45–57, 1973. 4, 28
- [14] E. Freire, E. Gamero, E. Ponce, and L.G. Franquelo. An algorithm for symbolic computation of center manifolds. In *Symbolic and algebraic computation (Rome, 1988)*, volume 358 of *Lecture Notes in Comput. Sci.*, pages 218–230. Springer, Berlin-New York, 1989. 10
- [15] J. Fujimura. Methods of centre manifold multiple scales in the theory of nonlinear stability for fluid motions. *Proc Roy Soc Lond A*, 434:719–733, 1991. 4
- [16] B. García-Archilla, J. Novo, and E.S. Titi. An approximate inertial manifolds approach to postprocessing the Galerkin method for the Navier-Stokes equations. *Maths. of Computation*, 68:893–911, 1999. 8, 42
- [17] B. García-Archilla and E.S. Titi. Postprocessing the Galerkin method: the finite element case. *SIAM J. Num. Anal.*, to appear:??, 1998. 9, 42
- [18] J. Guckenheimer and P. Holmes. *Nonlinear oscillations, dynamical systems, and bifurcations of vector fields*. Springer-Verlag, 1983. 31
- [19] M.S. Jolly. Explicit construction of an inertial manifold for a reaction diffusion equation. *J Diff Eqn*, 78:220–261, 1989. 3, 8

- [20] M.S. Jolly, I.G. Kevrekidis, and E.S. Titi. Approximate inertial manifolds for the Kuramoto-Sivashinsky equation: analysis and computations. *Physica D*, 44:38–60, 1990. 8
- [21] D.A. Jones, L.G. Margolin, and E.S. Titi. On the effectiveness of the approximate inertial manifold—a computational study. *Theoret. Comput. Fluid Dynamics*, 7:243–260, 1995. 8, 11
- [22] D.A. Jones and A.M. Stuart. Attractive invariant manifolds under approximation. Inertial manifolds. *J. Diff. Eqns*, 123:588–637, 1995. 8
- [23] T. Mackenzie and A.J. Roberts. Holistic finite differences accurately model the dynamics of the Kuramoto-Sivashinsky equation. Technical report, [<http://arXiv.org/abs/math.NA/0001079>], January 2000. 11
- [24] L.G. Margolin and D.A. Jones. An approximate inertial manifold for computing Burgers’ equation. *Physica D*, 60:175–184, 1992. 8
- [25] M. Marion and R. Temam. Nonlinear Galerkin methods. *SIAM J. Numer. Anal.*, 26(5):1139–1157, 1989. 8
- [26] G.N. Mercer and A.J. Roberts. A centre manifold description of contaminant dispersion in channels with varying flow properties. *SIAM J. Appl. Math.*, 50:1547–1565, 1990. 39
- [27] G.N. Mercer and A.J. Roberts. A complete model of shear dispersion in pipes. *Jap. J. Indust. Appl. Math.*, 11:499–521, 1994. 4
- [28] E. Meron and I. Procaccia. Theory of chaos in surface waves: The reduction from hydrodynamics to few-dimensional dynamics. *Phys. Rev. Lett.*, 56:1323–1326, 1986. 4
- [29] I. Procaccia. Universal properties of dynamically complex systems: the organisation of chaos. *Nature*, 333:618–623, 1988. 16th June. 4

- [30] R.H. Rand and W.L. Keith. Normal form and center manifold calculations on macsyma. In R. Pavelle, editor, *Applications of Computer Algebra*. Kluwer Acad, 1985. 10
- [31] A.J. Roberts. The application of centre manifold theory to the evolution of systems which vary slowly in space. *J. Austral. Math. Soc. B*, 29:480–500, 1988. 12
- [32] A.J. Roberts. Appropriate initial conditions for asymptotic descriptions of the long term evolution of dynamical systems. *J. Austral. Math. Soc. B*, 31:48–75, 1989. 10, 35
- [33] A.J. Roberts. The utility of an invariant manifold description of the evolution of a dynamical system. *SIAM J. Math. Anal.*, 20:1447–1458, 1989. 8
- [34] A.J. Roberts. Low-dimensional models of thin film fluid dynamics. *Phys. Letts. A*, 212:63–72, 1996. 4, 6, 15
- [35] A.J. Roberts. Low-dimensional modelling of dynamical systems. Technical report, [<http://arXiv.org/abs/chao-dyn/9705010>], 1997. 4
- [36] A.J. Roberts. Low-dimensional modelling of dynamics via computer algebra. *Comput. Phys. Comm.*, 100:215–230, 1997. 10, 16, 42
- [37] A.J. Roberts. An accurate model of thin 2d fluid flows with inertia on curved surfaces. In P.A. Tyvand, editor, *Free-surface flows with viscosity*, volume 16 of *Advances in Fluid Mechanics Series*, chapter 3, pages 69–88. Comput Mech Pub, 1998. 4
- [38] A.J. Roberts. Computer algebra derives correct initial conditions for low-dimensional dynamical models. *Comput. Phys. Comm.*, 1999. to appear. 10, 11, 35

- [39] A.J. Roberts. A holistic finite difference approach models linear dynamics consistently. Technical report, [<http://arXiv.org/abs/math.NA/0003135>], March 2000. 24, 29
- [40] J.C. Robinson. The asymptotic completeness of inertial manifolds. *Nonlinearity*, 9:1325–1340, 1996. 15
- [41] S. Rosencrans. Taylor dispersion in curved channels. *SIAM J. Appl. Math.*, 57:1216–1241, 1997. 4
- [42] G. Strang. A homework exercise in finite elements. *Int. J. Num. Meths Engrg*, 11:411–417, 1977. 9, 14
- [43] R. Temam. Inertial manifolds. *Mathematical Intelligencer*, 12:68–74, 1990. 8, 14
- [44] A. Vanderbauwhede. Centre manifolds. *Dynamics Reported*, pages 89–169, 1989. 14, 15
- [45] S.D. Watt and A.J. Roberts. The accurate dynamic modelling of contaminant dispersion in channels. *SIAM J Appl Math*, 55(4):1016–1038, 1995. 4